Computational Mechanics 17 (1995) 107–114 © Springer-Verlag 1995

New assumed strain triangles for non linear shell analysis*

F. G. Flores, E. Oñate, F. Zarate

Abstract A comparison between new and existing triangular finite elements based on the shell theory proposed by Juan Carlos Simo and co-workers is presented. Particular emphasis is put on the description of new triangles which show a promising behaviour for linear and non linear shell analysis.

1 Introduction

Considerable effort has been devoted in recent years to the development of efficient and reliable shell elements for linear and non linear analysis. Mainly two different approaches for the formulation of the elements have been used: the so called "degenerated solid" elements (Ahmad, Irons and Zienkiewicz 1970; Stanley, Park and Hughes 1986) and elements developed within the frame of a shell theory. Although the debate between "degenerate" versus "shell" formulation is still open, it is not the object of this work to discuss this subject. The interested reader is addressed to recent work of Büchter and Ramm (1992) and Büchter, Ramm and Roehl (1994) on this matter.

A general non linear shell theory very adequate for finite element computations has been recently proposed by Simo and Fox (1989), Simo, Fox and Rifai (1989, 1990), Simo, Rifai and Fox (1990) and Simo and Kennedy (1992) and excellent results were shown for the well known four node assumed shear strain quadrilateral. This fact motivated the authors to explore the possibilities of triangular elements based on this shell theory. Thus, the object of this work is to assess the behaviour of some linear assumed strain and quadratic triangular elements in the context of Simo's shell formulation. Particular emphasis is put on the extension of some successful assumed shear strain plate bending triangles developed by Oñate and Zienkiewicz, Suarez and Taylor (1992), Oñate, Zarate and Flores (1994) for linear and non linear shell analysis.

The layout of the paper is as follows. In next section a brief summary of Simo's shell theory is presented. Full details can be found in Simo and Fox (1989) and Simo, Fox and Rifai (1989). Then the different triangular shell elements analysed are described. Finally, examples of applications showing the performance of the triangular elements for some linear and non linear shell problems are given.

2 Summary of the shell theory chosen

A brief description of the shell theory developed by Simo and co-workers is presented here.

The configuration of the shell in $\mathbb{R}^3$ is defined by

a) the shell mid-surface $\boldsymbol{\varphi}$ defined by the transformation $\boldsymbol{\varphi}: \bar{\mathscr{A}} \to \mathbb{R}^3$
b) the director field $\mathbf{t}$ defined by the transformation $\mathbf{t}: \bar{\mathscr{A}} \to S^2$

Vector $\mathbf{t}$ defines the direction of the fibers across the thickness which remain straight during deformations (Fig. 1). The domain $\mathscr{A} \subset \mathbb{R}^2$ is assumed compact with smooth boundary $\partial\mathscr{A}$ and points characterized by $(\xi^1, \xi^2) \subset \bar{\mathscr{A}}$. Let us call $\partial_\varphi \subset \partial\mathscr{A}$ and $\partial_t\mathscr{A} \subset \partial\mathscr{A}$ the parts of $\partial\mathscr{A}$ with prescribed values of $\boldsymbol{\varphi}$ and $\mathbf{t}$, respectively. S^2 is the sphere with unit radius which contains $\mathbf{t}$, thus defining the inextensibility of the director field.

With this notation, the geometry of the shell can be defined by

$$\mathscr{S} := \{\mathbf{x} \in \mathbb{R}^3 / \mathbf{x} = \boldsymbol{\varphi} + \xi^3 \mathbf{t}, \xi^3 \in [h^-, h^+]\} \tag{1}$$

where $[h^-, h^+]$ defines the shell thickness. Using a standard basis $\{\mathbf{e}_1, \mathbf{e}_2, \mathbf{e}_3\}$ in $\mathbb{R}^3$ we can write (greek indices vary from 1 to 2)

$$\boldsymbol{\varphi} = \varphi^i \mathbf{e}_i \quad \boldsymbol{\varphi}'_\alpha = \varphi^i_{,\alpha} \mathbf{e}_i \quad \mathbf{t} = t^i \mathbf{e}_i \tag{2}$$

The following measures over the mid-surface are defined

$$d\mu^0 = \bar{j}^0 d\xi^1 d\xi^2 \quad d\mu = \bar{j} d\xi^1 d\xi^2 \tag{3}$$

with

$$\bar{j}^0 = (\boldsymbol{\varphi}'^0_1 \times \boldsymbol{\varphi}'^0_2) \cdot \mathbf{t}^0 \quad \bar{j} = (\boldsymbol{\varphi}'_1 \times \boldsymbol{\varphi}'_2) \cdot \mathbf{t} \tag{4}$$

and

$$\bar{J} = \bar{j}/\bar{j}^0 \tag{5}$$

Communicated by S. N. Atluri, 18 August 1995

F. G. Flores
CONICET Staff Member, Department of Structures, National University of Córdoba, Casilla de Correo 916, 5000 Córdoba, Argentina

E. Oñate, F. Zarate
E.T.S. Ingenieros de Caminos, Canales y Puertos Universidad Politécnica de Cataluña c/ Gran Capitán s/n 08034 Barcelona, Spain

Correspondence to: F. G. Flores

F. Flores was supported by a fellowship from the Spanish Government during the development to this work. This support is gratefully acknowledged.

* In memoriam of Juan Carlos Simo

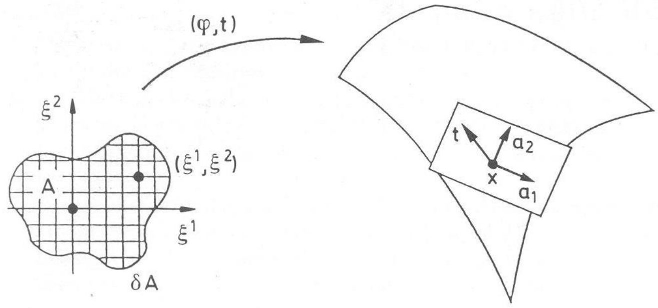

Fig. 1. Basic definition of shell geometry

In (3–5), $(\cdot)^0$ denotes geometrical variables associated with the reference configuration $\mathscr{S}^0$.

A convective system is now defined over the deformed and reference configurations as

$$\{\boldsymbol{\varphi}'_{\alpha}, \mathbf{t}\} \equiv \{\mathbf{a}_{\alpha}, \mathbf{a}_3\}, \quad \{\boldsymbol{\varphi}^0_{,\alpha}, \mathbf{t}^0\} \equiv \{\mathbf{a}^0_{\alpha}, \mathbf{a}^0_3\} \tag{6}$$

The deformation gradient over the mid-surface ($\xi^3 = 0$) in $\mathbf{x}^0_0 = \boldsymbol{\varphi}^0(\xi^1, \xi^2)$ is given by the linear appplication

$$\bar{\mathbf{F}} := \mathbf{a}_{\alpha} \otimes \mathbf{a}^{0\alpha} + \mathbf{t} \otimes \mathbf{a}^{03} \equiv \mathbf{a}_i \otimes \mathbf{a}^{0i} \tag{7}$$

The following tensors defining the metric of the system are defined on the actual configuration

$$a_{\alpha\beta} = \mathbf{a}_{\alpha} \cdot \mathbf{a}_{\beta} \tag{8}$$

$$\gamma_{\alpha} = \boldsymbol{\varphi}'_{\alpha} \cdot \mathbf{t} \tag{9}$$

$$\kappa_{\alpha\beta} = \boldsymbol{\varphi}'_{\alpha} \cdot \mathbf{t}_{,\beta} \tag{10}$$

Using identical definitions for the reference configuration $\mathscr{S}^0$, the following generalized Lagrangian strains can be defined

a) *Mid-surface strains*

$$\boldsymbol{\varepsilon}(\boldsymbol{\varphi}) = \frac{1}{2}\begin{bmatrix} a_{11} - a^0_{11} \\ a_{22} - a^0_{22} \\ 2(a_{12} - a^0_{12}) \end{bmatrix} \tag{11}$$

b) *Transverse shear strains*

$$\boldsymbol{\delta}(\boldsymbol{\varphi}, \mathbf{t}) = \begin{bmatrix} \gamma_1 - \gamma^0_1 \\ \gamma_2 - \gamma^0_2 \end{bmatrix} \tag{12}$$

c) *Curvature strains*

$$\boldsymbol{\chi}(\boldsymbol{\varphi}, \mathbf{t}) = \begin{bmatrix} \kappa_{11} - \kappa^0_{11} \\ \kappa_{22} - \kappa^0_{22} \\ 2(\kappa_{12} - \kappa^0_{12}) \end{bmatrix} \tag{13}$$

The resultant stresses can be written in terms of stress measures over the deformed or current configurations as

$$\mathbf{n}^{\alpha} = \frac{1}{j}\int_{h^-}^{h^+} \boldsymbol{\sigma}\mathbf{g}^{\alpha} j d\xi^3 = \frac{1}{j}\int_{h^-}^{h^+} \mathbf{P}\mathbf{g}^{\alpha}_0 j^0 d\xi^3 \tag{14}$$

$$\mathbf{m}^{\alpha} = \mathbf{t} \times \frac{1}{j}\int_{h^-}^{h^+} \xi^3 \boldsymbol{\sigma}\mathbf{g}^{\alpha} j d\xi^3 = \mathbf{t} \times \frac{1}{j}\int_{h^-}^{h^+} \xi^3 \mathbf{P}\mathbf{g}^{\alpha}_0 j^0 d\xi = \mathbf{t} \times \tilde{\mathbf{m}}^{\alpha} \tag{15}$$

$$\mathbf{l} = \frac{1}{j}\int_{h^-}^{h^+} \boldsymbol{\sigma}\mathbf{g}^3 j d\xi^3 = \frac{1}{j}\int_{h^-}^{h^+} \mathbf{P}\mathbf{g}^3_0 j^0 d\xi \tag{16}$$

where $\mathbf{g}^i = \partial\mathbf{x}/\partial\xi^i$. $\boldsymbol{\sigma}$ and $\mathbf{P}$ are the Cauchy and 1st Piola-Kirchhoff stress tensors, respectively. On the other hand $\mathbf{n}^{\alpha}$ and $\mathbf{m}^{\alpha}$ are the resultant stresses and bending moments along a line $\xi^{\alpha} =$ constant and $\mathbf{l}$ is the resultant stress across the thickness. Vector $\tilde{\mathbf{m}}^{\alpha}$ is termed "director bending moment" and it allows to define the following "effective resultant stresses" as

$$\tilde{n}^{\beta\alpha} := n^{\beta\alpha} - \lambda^{\beta}_{\mu}\tilde{m}^{\alpha\mu} \tag{17}$$

$$\tilde{q}^{\alpha} := q^{\alpha} - \lambda^3_{\mu}\tilde{m}^{\alpha\mu} \tag{18}$$

where λ^M_{α} and λ^3_{α} are obtained from the relationship

$$\mathbf{t}_{,\alpha} = \lambda^{\mu}_{\alpha}\boldsymbol{\varphi}'_{\mu} + \lambda^3_{\alpha}\mathbf{t} \tag{19}$$

It can be shown that the resultant stresses $\tilde{\mathbf{m}}^{\alpha}$, $\tilde{\mathbf{n}}^{\alpha}$ and $\tilde{\mathbf{q}}^{\alpha}$ are conjugate of the generalized strains defined in (11–13). The constitutive equation between both sets of magnitudes can be written as

$$\tilde{n}^{\beta\alpha} = \bar{\rho}\frac{\partial\psi}{\partial\varepsilon_{\beta\alpha}} \quad \tilde{q}^{\alpha} = \bar{\rho}\frac{\partial\psi}{\partial\delta_{\alpha}} \quad \tilde{m}^{\beta\alpha} = \bar{\rho}\frac{\partial\psi}{\partial\chi_{\beta\alpha}} \tag{20}$$

where ψ is the internal energy and

$$\bar{\rho} = \frac{1}{j}\int_{h^-}^{h^+} \rho j d\xi^3 \tag{21}$$

ρ being the material density. Details on the constitutive relationship for both elasticity and elasto-plasticity using an hyperelastic framework can be found in Simo and Fox (1989) and Simo and Kennedy (1992).

The expression of the internal stress power due to deformation can be written as

$$\begin{aligned} \mathscr{W} &:= \int_{\mathscr{V}} \mathbf{P} : \dot{\mathbf{F}}\, d\mathscr{V} \\ &= \int_{\mathscr{A}} [\mathbf{n}^{\alpha} \cdot \dot{\boldsymbol{\varphi}}'_{\alpha} + \tilde{\mathbf{m}}^{\alpha} \cdot \dot{\mathbf{t}}_{,\alpha} + \mathbf{l} \cdot \dot{\mathbf{t}}]\, d\mu \\ &= \int_{\mathscr{A}} [\tilde{n}^{\beta\alpha}\tfrac{1}{2}\dot{a}_{\beta\alpha} + \tilde{q}^{\alpha}\dot{\gamma}_{\alpha} + \tilde{m}^{\alpha\beta}\dot{\kappa}_{\beta\alpha}]\, d\mu \\ &= \int_{\mathscr{A}} [\tilde{\mathbf{n}} : L_u\boldsymbol{\varepsilon} + \tilde{\mathbf{q}} : L_u\boldsymbol{\delta} + \tilde{\mathbf{m}} : L_u\boldsymbol{\chi}]\, d\mu \end{aligned} \tag{22}$$

Equation (22) is the basis for the derivation of the finite element formulations following standard procedures. This requires the definition of adequate admissible variations

($\delta\boldsymbol{\varphi}, \delta\mathbf{t}$) (Simo and Fox 1989). Note that the requirements of inextensibility of $\mathbf{t}$ lead to the well known relationship

$$\underset{(3\times 1)}{\delta\mathbf{t}} = \underset{(3\times 2)}{\bar{\boldsymbol{\Lambda}}} \underset{(2\times 1)}{\delta\mathbf{T}} \tag{23}$$

where $\bar{\boldsymbol{\Lambda}}$ contains the first two rows of the orthogonal matrix which transforms the global vector $\mathbf{e}_3$ into $\mathbf{t}$ and $\delta\mathbf{T} = [\delta T_1, \delta T_2]^T$. Equation (23) can be written in a more convenient form as

$$\delta\mathbf{t} = \delta\boldsymbol{\theta} \times \mathbf{t} \tag{24}$$

where $\delta\boldsymbol{\theta}$ is a vector normal to the plane formed by $\mathbf{t}$ and $\delta\mathbf{t}$, i.e. $\delta\boldsymbol{\theta}\cdot\mathbf{t} = 0$.

3
Description of new triangular shell elements

3.1
Six node quadratic shell triangle with linear assumed transverse shear (TQQL element)

This element is an extension of the quadratic plate triangle presented in Zienkiewicz, Taylor, Papadopoulos and Oñate (1990) and Oñate, Zienkiewicz, Suarez and Taylor (1992). The geometry of the element is shown in Fig. 2. Both initially flat (subparametric) and curved (isoparametric) versions of the element have been considered. In the subparametric case, the initial geometry is *linearly* interpolated in terms of the vertex nodal values, whereas a quadratic approximation is used in the isoparametric case. For flat triangles the jacobian matrix is constant which considerably simplifies some computations. In both flat and curved cases the displacement and director fields are quadratically interpolated as

$$\mathbf{u} = \sum_{I=1}^{6} N^I \mathbf{u}^I$$

$$\tilde{\mathbf{t}}^0 = \sum_{I=1}^{6} N^I \mathbf{t}^I \quad \text{with} \quad \mathbf{t} = \frac{\tilde{\mathbf{t}}}{\|\tilde{\mathbf{t}}\|} \tag{25}$$

where N^I are the quadratic shape functions of the standard six node C_0 triangle (Zienkiewicz and Taylor 1989/1991).

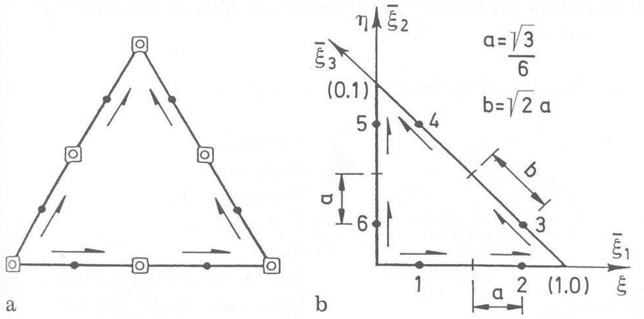

Fig. 2a–b. TQQL shell triangle (a) nodal points with degrees of freedoms [$u, \Delta\mathrm{T}$], (b) sampling points for the tangential transverse shear strain γ_t

The updated middle surface configuration and the director field are obtained for step $k+1$ by

$$\boldsymbol{\varphi}^{k+1} = \sum_{I=1}^{6} N^I(\xi,\eta)(\boldsymbol{\varphi}_I^0 + \mathbf{u}_I^{k+1}) \tag{26}$$

$$\mathbf{t}^{k+1} = \sum_{I=1}^{6} N^I(\xi,\eta)\mathbf{t}_I^{k+1} \tag{27}$$

with

$$\mathbf{t}_I^{k+1} = \exp_{t_I^k}[\Delta\mathbf{t}_I^k] := \cos(\|\Delta\mathbf{t}_I^k\|)\,\mathbf{t}_I^k + \frac{\sin(\|\Delta\mathbf{t}_I^k\|)}{\|\Delta\mathbf{t}_I^k\|}\Delta\mathbf{t}_I^k \tag{28}$$

Note that $\Delta\mathbf{t}_I^k$ is the increment between steps k and $k+1$.

The local axes in this element have been defined as follows. Axis $\mathbf{x}_3$ is taken orthogonal to the element plane; $\mathbf{x}_1$ is assumed to lay in the intersection of the element with the global $\mathbf{x}_1$, $\mathbf{x}_2$ plane and $\mathbf{x}_2 = \mathbf{x}_3 \times \mathbf{x}_1$.

Two versions of the element have been studied in this work. The first one is based on the standard displacement formulation for both bending and membrane fields whereas a linear transverse shear strain field is assumed in the natural coordinate system as

$$\gamma_\xi = \alpha_1 + \alpha_2\xi + \alpha_3\eta$$
$$\gamma_\eta = \alpha_4 + \alpha_5\xi + \alpha_6\eta \tag{29}$$

Parameters $\alpha_1 \cdots \alpha_6$ are obtained by sampling the tangential shears in the six side points shown in Fig. 2b. The derivation of the substitute (B-bar)transverse shear strain matrix for this case follows the lines explained in Oñate, Zienkiewicz, Suárez and Taylor (1992). Further details are given in Flores and Oñate (1993). Following the notation of Oñate et al. (1992) this element is termed here TQQL (For Triangle, Quadratic displacements, Quadratic rotations and Linear assumed transverse shear fields). The flat version of this element is termed TQQL$_f$, whereas TQQL denotes the curved isoparametric version.

For the isoparametric (curved) case, a second version of this element uses the following assumed membrane field (aimed to avoid membrane locking)

$$\bar{\boldsymbol{\varepsilon}}'(\xi,\eta) = \begin{bmatrix} \varepsilon_{\xi\xi} \\ \varepsilon_{\eta\eta} \\ 2\varepsilon_{\xi\eta} \end{bmatrix} = \begin{bmatrix} 1 & \xi & \eta & & & & & & \\ & & & 1 & \xi & \eta & & & \\ & & & & & & 1 & \xi & \eta \end{bmatrix} \cdot \begin{bmatrix} \beta_1 \\ \beta_2 \\ \cdots \\ \beta_9 \end{bmatrix} = \mathbf{A}(\xi,\eta)\beta \tag{30}$$

where the parameters $\beta_1 \cdots \beta_9$ are obtained by sampling the membrane strains at selected points. Two possibilities have been considered: (i) evaluating the assumed membrane strains at the vertex nodes (element TQQL1) and (ii) evaluating the tangential membrane strains at the two Gauss points along each side and additionally sampling the three membrane strains at the center of the element (element TQQL2). Details of the finite element matrices necessary for non linear computation can be found in Flores and Oñate (1993).

3.2
Linear/quadratic shell triangle with a linear assumed shear strain field (TLQL element)

This element is an extension of the TLQL plate triangle presented in Zienkiewicz, Taylor, Papadopoulos and Oñate (1990) and also in Oñate, Zienkiewicz, Suarez and Taylor (1992). The mid-surface displacements are now *linearly* interpolated in the terms of the corner values as

$$\mathbf{u} = \sum_{I=1}^{3} \xi^I \mathbf{u}^I \tag{31}$$

whereas the following incomplete *quadratic* approximation is used for the director field

$$\tilde{\mathbf{t}} = \sum_{I=1}^{3} \xi^I \mathbf{t}^I + \sum_{I=4}^{6} N^I \theta^I \mathbf{e}^I \tag{32}$$

In (31) and (32) ξ^I are the standard linear shape functions of the 3 node triangle, N^I are the standard quadratic shape functions for the 6 node triangle and θ^I are hierarchical director values. In the plate bending case $\mathbf{e}^I$ are side vectors, whereas in this case we have taken

$$\mathbf{e}^4 = (\boldsymbol{\varphi}^2 + \mathbf{t}^2) - (\boldsymbol{\varphi}^1 + \mathbf{t}^1)$$

$$\mathbf{e}^5 = (\boldsymbol{\varphi}^3 + \mathbf{t}^3) - (\boldsymbol{\varphi}^2 + \mathbf{t}^2) \tag{33}$$

$$\mathbf{e}^6 = (\boldsymbol{\varphi}^1 + \mathbf{t}^1) - (\boldsymbol{\varphi}^3 + \mathbf{t}^3)$$

Note that vectors $\mathbf{e}^I$ must be updated at every solution step. In this way we ensure a smooth director field along each side.

The bending and membrane contributions are obtained in a straightforward manner using a standard displacement formulation. Finally, the transverse shear strain field is assumed to vary linearly in terms of the three tangential shear strains at the side-points shown in Fig. 3. The derivation of the substitute shear strain matrix follows the lines explained in Oñate, Zienkiewicz, Suarez and Taylor (1992) for the analogous plate element and it will not be repeated here.

3.3
Linear shell triangle with linear assumed shear strains (TLLL element)

This element is an extension of the TLLL plate element recently proposed by Oñate, Zarate and Flores (1994). Now the displacement and rotation fields and the assumed transverse shear strains are *linearly* interpolated in terms of the vertex *nodal* displacements, the *mid-side rotations* (defining an incompatible rotation field) and the *mid-side* tangential shear strain variables, respectively as shown in Fig. 4. Note that the assumed shear field for this element is identical to that of the TLQL of previous section.

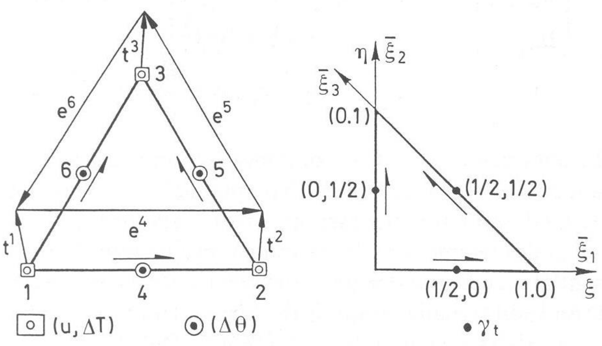

Fig. 3. TLQL triangular shell element. Nodes and sampling points for the tangential transverse shear strain γ_t

The director field is interpolated in terms of the director vectors at the mid-side nodes as

$$\tilde{\mathbf{t}} = \sum_{I=4}^{6} N^I \mathbf{t}^I \tag{34}$$

where

$$N^I = 1 - 2\xi^I \tag{35}$$

with ξ^I being the standard linear shape functions of the 3 node triangle.

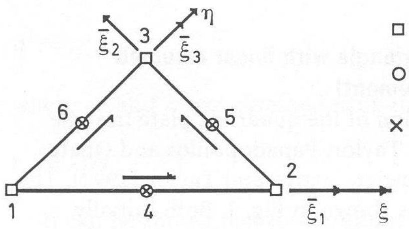

Fig. 4. TLLL triangular shell element. Nodes and sampling points for the tangential transverse shear strain γ_t

It is worth noting that many interesting analogies can be found between this element and that derived by Van Keulen (1993) (see also Van Keulen and Oñate, 1995) as an extension of the well known 6 dof triangle developed by Morley (1971). More details about the derivation of the element matrices for the TLLL element can be found in Oñate, Zarate and Flores (1994) and in Flores and Oñate (1993).

4
Examples

4.1
Cylindrical roof

The well known Scordelis-Lo cylindrical roof shown in Fig. 5 is chosen first to compare the behaviour of the triangular shell elements previously described with that of the popular

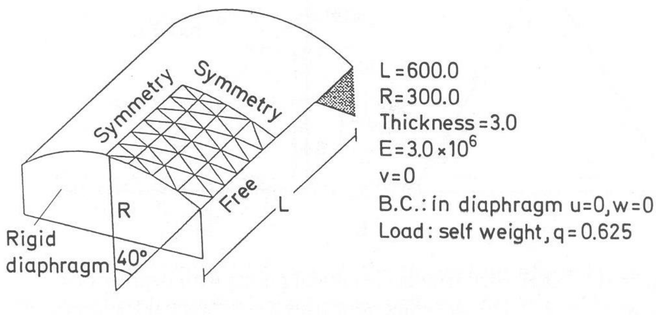

Fig. 5. Scordelis-Lo cylindrical roof. Geometry and material properties

DOF	QLLL	$TQQL_f$	TQQL	TQQL1	TQQL2	DOF	TLQL	DOF	TLLL
92	1.083	1.349	0.544	1.121	0.484	42	1.135	42	1.479
198	–	1.095	0.747	1.007	0.694	87	0.745	90	0.800
344	1.015	1.044	0.872	0.983	0.860	148	0.742	156	0.762
1344	1.000	–	–	–	–	850	0.916	930	0.920
2060	–	1.005	0.994	1.003	1.000	3500	0.977	3660	0.977

Table 1. Convergence of the vertical displacement at the mid-side point of the edge

four noded quadrilateral with linearly assumed transverse shear strains (termed here QLLL) (Dvorkin and Bathe 1984; Simo, Fox and Rifai 1989; Oñate, Zienkiewicz, Suarez and Taylor 1992).

Table 1 shows the convergence of the normalized vertical displacements of the free edge of the central section for different meshes. Elements TQQL and TQQL2 show slow convergence due to membrane locking. Element $TQQL_f$ converges to the correct result but it is rather flexible.

4.2
Curved cantilever beam

A popular example to evaluate membrane locking behaviour of curved elements is the uniform bending of a curved cantilever. The basic geometry and material data are shown in Fig. 6. Numerical results have been obtained for different values of the span angle ϕ. The normalized bending moments at the Gauss points for the different shell triangles are presented in Table 2. Note the low performance of the displacement-based element TQQL for increasing values of ϕ.

4.3
Roll-up of clamped beam

A clamped-free slender strip is subjected to a bending moment at the free edge and it is deformed into a circular arc of radius ρ given by the relation

$$\kappa = \frac{1}{\rho} = \frac{M}{EI}$$

Using a displacement control Newton-Raphson algorithm (in this case the rotation of the free edge is taken as the control d.o.f.) the shell is deformed into a complete circle (Fig. 7). The value of the normalized applied bending moment for the different triangular elements is presented in Table 3.

4.4
Hinged cylindrical panel under a point load

A shallow cylindrical panel, pinned at two edges and free at the other two, subjected to a central point load leads to

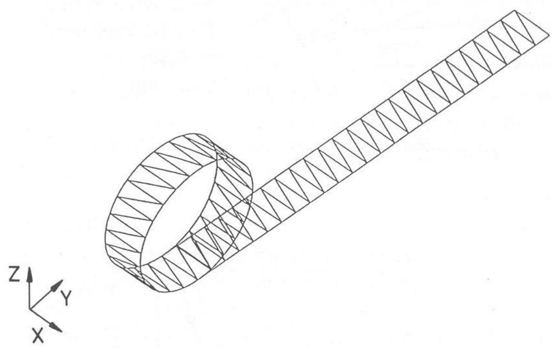

Fig. 7. Roll-up of a clamped strip. Reference and deformed configurations

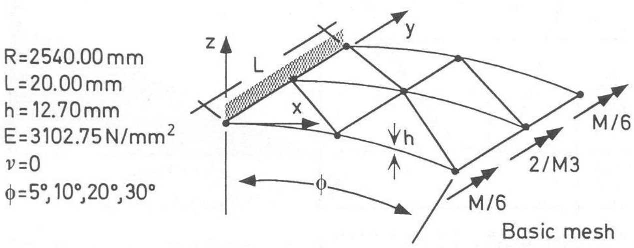

Fig. 6. Cantilever curved beam. Geometry and material properties

Table 3. Roll-up a clamped beam. Normalized bending moment for a complete circle configuration

$TQQL_f$, TQQL	TQQL1	TQQL2	TLQL	TLLL
1.002	0.980	1.016	0.990	0.989

ϕ	TQQL	TQQL1	TQQL2	TLQL	TLLL
5	0.992	1.001	1.000	1.0093	1.0095
10	0.878–0.920	1.005	0.998	1.0052–1.0023	1.0053–1.0022
20	0.408–0.710	1.020	0.990–0.996	1.014–1.016	1.0158–1.0155
30	0.244–0.615	1.038–1.048	0.978–0.991	1.036–1.034	1.0374–1.0356

Table 2. Curved cantilever beam. Bending moment at Gauss points. Numbers show the range of variation of bending moment values in the mesh. Exact solution is 1.0

a snap-through behaviour with a reversal of curvature. Depending on the thickness a snap-back is also possible. Two different thicknesses have been considered for $R/h = 200$ and $R/h = 400$. The geometry of the panel and the material properties are shown in Fig. 7. For $R/h = 200$ two regular meshes (25 and 49 nodes) have been used to test convergence. The displacement of the point under the load vs. the value of the load is plotted in Fig. 9 for the triangular elements presented here. It can be seen that for the fine mesh (Fig. 9b) the results are almost coincident and all elements converge to the correct results. Results for the case $R/h = 400$ using the fine mesh are presented in Fig. 10. The TQQL1 element shows a very flexible behaviour in this case.

4.5
Impact dynamics test

The triangular shell elements proposed seem particularly advantageous for crashworthiness and sheet stamping problems where the triangular discretization of complex shell geometries is typically required.

A simple example of the ability of the shell triangles for analysis of impact dynamics problem presented is given here.

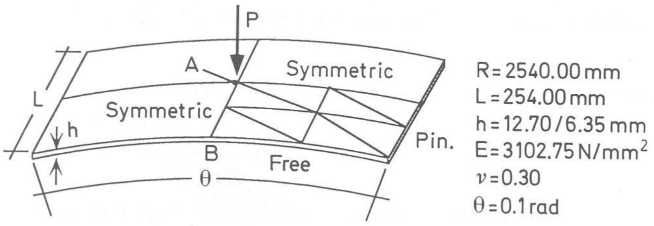

Fig. 8. Hinged Cylindrical Panel, geometry and material properties

The problem is the study of the impact of a low-velocity ($V_0 = 6.94$ m/s) cylindrical bar against a clamped square plate (Hallet 1987). The plate dimensions are 600×600 mm and the thickness is 5.11 mm, whilst the projectile has a diameter of 40 mm and a mass of 40.5 kg. Interface conditions are frictionless and the material properties for both target and projectile are $E = 211 \times 10^9$ N/m², $\nu = 0.3$, *initial yield stress* = 280×10^6 N/m² and *hardening modulus* = 690×10^6 N/m². The elastoplastic model used is described in Simo and Kennedy (1993).

Due to symmetry conditioning an eighth of the plate is considered. Six finite strain 8-node solid elements (Garcia Garino 1993) have been used for the projectile and 24 TQQL shell triangles for the plate. Vertical displacement contours are shown in Fig. 11 for the instant of maximum deformation. Also the displacements of the center of the plate and the blunt surface of the projectile are plot with respect to time. The maximum displacement of the plate was computed as 27.5 mm at 6.3 ms in comparison with the experimental values of 27.6 mm at 5.47 ms which represents errors of − 0.4% and 14.5% respectively. Similar good behaviour was found for the TLQL and TLLL elements. Further details on this example and other non linear dynamic studies using the new shell triangles can be found in Flores and Oñate (1993).

5
Concluding remarks

A family of assumed strain triangles for non linear thick/thin shell analysis has been presented. The elements follow the shell theory by Simo and co-workers and can deal with large displacements, large rotations and plasticity effects.

All the elements converge to the correct results when the mesh is refined. For coarse meshes it has been observed that:

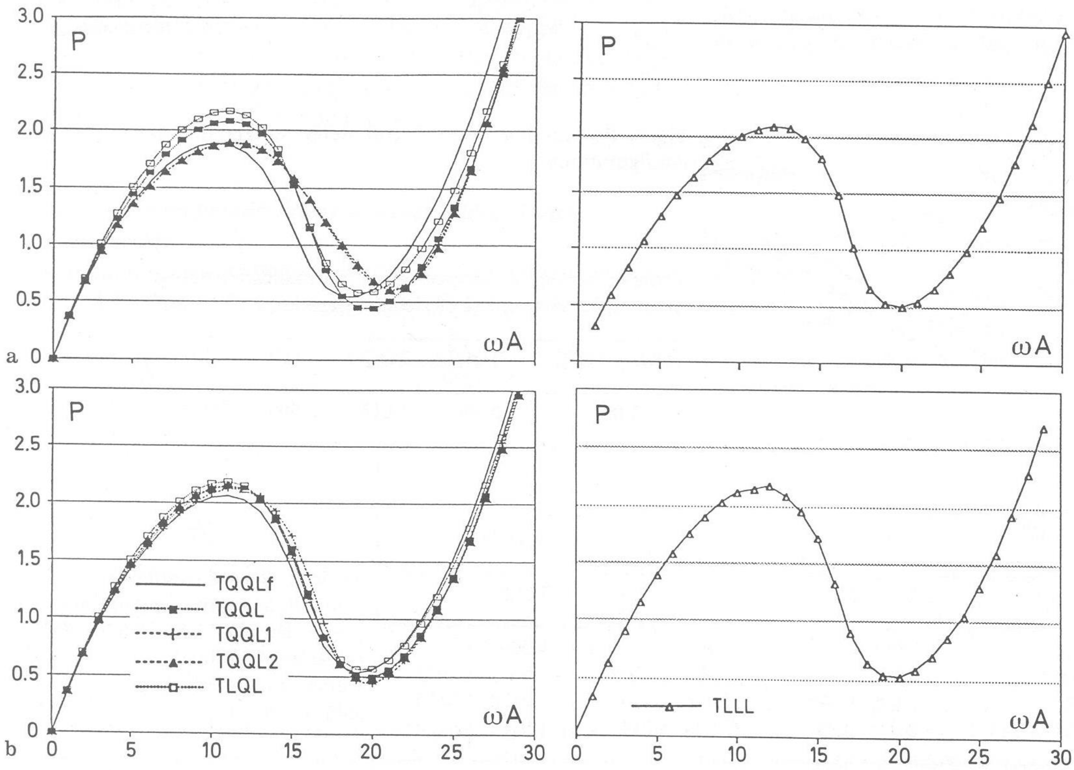

Fig. 9a–b. Hinged cylindrical panel, $R/h = 200$, displacement under load (w) versus load P, (**a**) 5×5 mesh, (**b**) 7×7 mesh

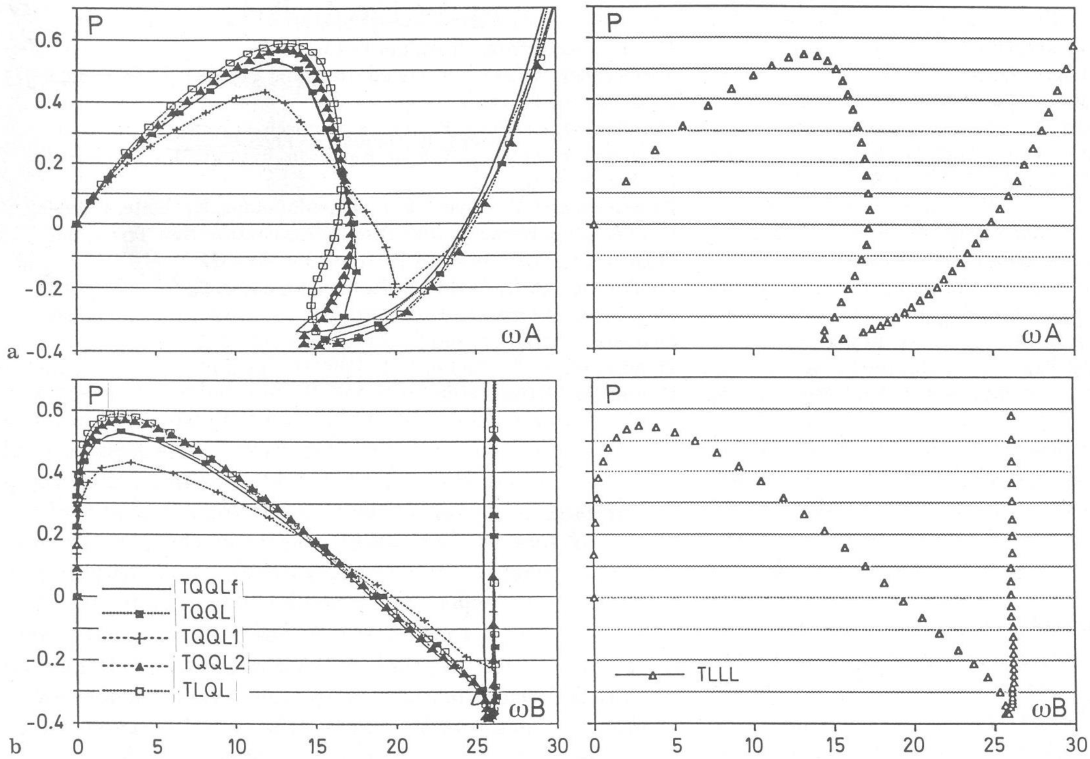

Fig. 10a–b. Hinged cylindrical panel, $R/h = 400$, 7×7 mesh (**a**) displacement of the central point (w_A) versus load, (**b**) displacement at mid point of the free edge (w_B) versus load

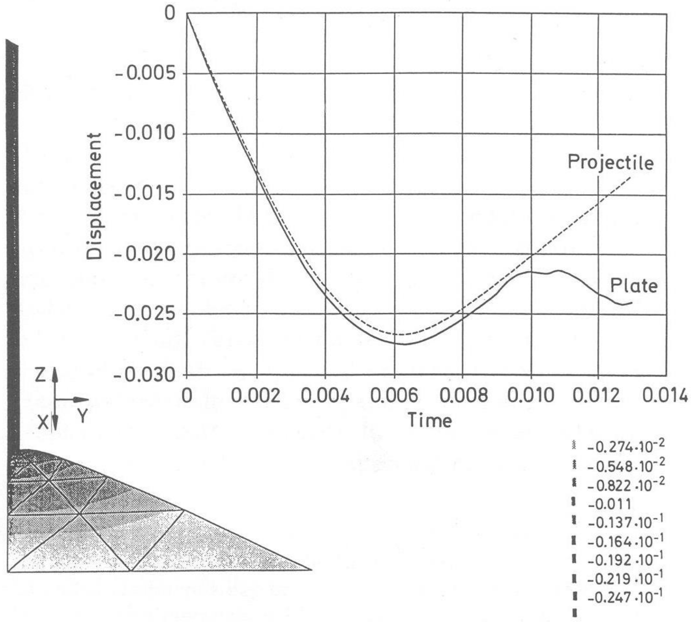

Fig. 11. Impact of a metallic bar against a square plate. Evolution of central displacement: continuous line (—) for plate and dashed (- -) for projectile. Displacement contours for $t = 0.006$

(a) Both the flat $TQQL_f$ element and the assumed membrane strain TQQL1 element behave rather flexible.
(b) The isoparametric TQQL element exhibits membrane locking as expected.
(c) The TQQL2 element with assumed membrane strains behaves rather stiff.
(d) The TLQL element has an excellent bending behaviour but for membrane dominated problems requires fine meshes due to the intrinsic constant membrane strain field.
(e) The TLLL exhibits a behaviour similar to that of the TLQL element although its formulation is much simpler. Indeed this element is a promising candidate for large scale non linear computations of shells.

References

Ahmad, S.; Irons, B. M.; Zienkiewicz, O. C. 1970: Analysis of thick and thin shell structures by curved finite elements. Int. J. Num. Methds. in Eng. 2: 419–451

Bûchter, N.; Ramm, E. 1992: Shell theory versus degeneration. A comparison in large rotation finite element analysis. Int. J. Num. Methds. in Eng. 34: 39–59

Büchter, N.; Roehl, D.; Ramm, E. 1994: Three dimensional extension of non-linear shell formulation based on the enhanced assumed strain concept. Int. J. Num. Methds. in Eng. 37: 2251–2568

Dvorkin, N.; Bathe, K. J. 1989: A continuum mechanics based, four noded shell element for non-linear analysis. Eng. Comput., 1: 77–88

Flores, F.; Oñate, E. 1993: A Comparison of Different Finite Elements based on Simo's Shell Theory, (in Spanish), Research Report, 33: CIMNE, Barcelona

Flores, F.; Oñate, E. 1993: Dynamic analysis of shells and rods (in Spanish) Research Report 39: CIMNE, Barcelona

García Garino, C. 1993: A Numerical Model for Large Strain Analysis of Elasto-plastic Solids, Ph.D. Thesis (in Spanish) Universidad Politécnica de Cataluña

Hallet, N. 1987: Large Deflection Impulsive Loading of Plates, Ph.D. Thesis, City University, London

Morley, L. S. D. 1971: The constant moment plate bending element. J. Strain Anal., 6: 20–24

Oñate, E.; Zarate, F.; Flores, F. 1994: A simple triangular element for thick and thin plate and shell analysis. Int. J. Num. Methds. in Eng. 37: 2569–2582, 1994

Oñate, E.; Zienkiewicz, O. C.; Suarez, B.; Taylor, R. L. 1992: A General Methodology for Deriving Shear-Constrained Reissner-Mindlin Plate Elements. Int. J. Num. Methds. in Eng.

Simo, J. C.; Fox, D. D. 1989: On Stress Resultant Geometrically Exact Shell Model. Part I: Formulation and Optimal Parametrization, Comput. Meths. Appl. Mech. Engrg. 72: 267–304

Simo, J. C.; Fox, D. D.; Rifai, M. S. 1989: On Stress Resultant Geometrically Exact Shell Model. Part II: The Linear Theory; Computational Aspects, Comput. Meths. Appl. Mech. Engrg. 73: 53–92

Simo, J. C.; Fox, D. D.; Rifai, M. S. 1990: On Stress Resultant Geometrically Exact Shell Model. Part III: Computational Aspects of The Nonlinear Theory. Comput. Meths. Appl. Mech. Engrg. 79: 21–70

Simo, J. C.; Kennedy, J. G. 1992: On Stress Resultant Geometrically Exact Shell Model. Part IV Nonlinear Plasticity: formulation and integration algorithms. Comput. Meths. Appl. Mech. Engrg. 96: 133–171

Simo, J. C.; Rifai, M. S.; Fox, D. D. 1990: On Stress Resultant Geometrically Exact Shell Model. Part IV: Variable thickness shells with through the thickness stretching. Comput. Meths. Appl. Mech. Engrg. 81: 91–126

Stanley, G. M.; Park, K. C.; Hughes, T. J. R. 1986: Continuum-Based Resultant Shell Elements. In Finite Element Methods for Plate and Shell Structures, Vol. 1: Element Technology, (Ed. T. J. R. Hughes & E. Hinton) Pineridge Press, pp. 1–45

Van Keulen, F. 1993: On refined triangular plate and shell elements, Ph.D. Thesis, TU Delft

Van Keulen, F.; Oñate, E. 1995: A comparison between two a dof triangles for thick and thin plate analysis. Submitted to Int. J. Num. Methds. in Eng.

Zienkiewicz, O. C.; Taylor, R. L.; Papadopoulos, P.; Oñate, E. 1990: Plate Bending Elements with Discrete Constrains: New Triangular Elements. Computers and Structures, 35: 505–522
Zienkiewicz, O. C.; Taylor, R. L.; Papadopoulos, P.; Oñate, E. 1990: Plate Bending Elements with Discrete Constrains: New Triangular Elements. Computers and Structures, 35: 505–522
Zienkiewicz, O. C.; Taylor, R. L. 1989/91: The finite element method, IV Edition, McGraw-Hill, Vol. I, Vol. II